6 In-Vitro mucus penetration studies of antigen conjugated Nanoparticles

6.1 Mucus

Mucus is a viscoelastic and adhesive gel that protects the lung airways, gastrointestinal (GI) tract, vagina, eye and other mucosal surfaces. The gross composition of mucus is about 1% by weight of salts and other dialyzable components, 0.5 – 1% by weight of free protein, 0.5 – 1% by weight of carbohydrate-rich glycoproteins called mucin and 95% and above water. Mucins are large molecules, typically 0.5 to 40 MDa in size (Singh 2002) formed by linking of numerous mucin monomers and are coated with complex and highly diverse array of proteoglycans. The pH of mucus varies greatly with mucosal surface: Lung and nasal mucus are neutral in pH, vaginal mucus is acidic (pH ~ 4) and eye mucus is slightly alkaline (pH ~ 7.8). The thickness of mucus layer varies from 0.03 (eye) to 200μm (gastric) mucosal site (Lai 2009).

At least twenty glycoproteins have been assigned to the *MUC* gene family (Dekker 2002, Ali 2007) with several mucin types expressed at each mucosal surface (Corfield 2001, Gipson 2001, Rubin 2002, Ali 2007). Mucin can be classified into two categories: cell associated mucin and secreted mucin. In addition to mucins, mucus gels are loaded with cells, bacteria, lipids, salts proteins, macromolecules and cellular debris. The various components work together to form a nano-scopically heterogeneous environment with a shear dependent bulk viscosity in the range of 1000-10,000 times higher than the viscosity of water at low shear rates. Mucus visco-elasticity is tightly regulated in healthy subject by controlling the mucin to water secretion ratio (Wolf 1977) as well as by varying lipid (Galabert 1987), protein (Girod 1992), and ion content (Raynal 2003). Mucus is continuously secreted, then shed and discarded/ digested/ recycled.

[1] Declaration:

[1] This work is carried out under the guidance of Dr. Justin Hanes, Professor, Johns Hopkins University (JHU), Baltimore, MD-USA. Heena Soni has official collaboration for her doctoral work with his Nano-medicine group at Johns Hopkins University, USA. JHU has licensed the mucus penetrating particle technology (MPP) to Kala Pharmaceuticals, MA, USA.

The mucus clearance time is short. Rate of mucus clearance varies from one site to another with different mechanisms acting on those sites. The understanding of mucus layer thickness, clearance time and mechanism of clearance is the key for designing drug delivery system for that site. The bottom line for designing delivery system through mucus is remaining on the fact that the rate of particle diffusion through the mucus layer should be higher than the rate of mucus clearance (Lai 2009).

6.2 Mucus Penetrating Particles

The bulk viscosity of healthy human mucus at low shear rate is about 1000 to 10,000 times higher than the viscosity of water. According to Stokes' Law for diffusion in homologues fluids, it is indicated that at this viscosity, macromolecule penetration is impossible. However, Saltzman and Cone (1994) showed that diffusion of various proteins and antibodies, in human cervical mucus was unhindered relative to their rates in water. The same studies showed penetration of virus less than 30 nm was unhindered and later the study was supported by Olmsted (2001). Finally, it was established that small particles are capable of diffusing through low viscosity pores within the highly elastic mucin fiber matrix. The viscosity of the fluid that fills the pores in mucus is equivalent to that of water, so the transport of non-mucoadhesive particles is expected to be similar to their rates in water (Lai 2010).

The primary mechanism of trapping pathogens in mucus can be explained by formation of polyvalent adhesive interaction. The high density of hydrophobic domains, coupled with the flexible nature of mucins facilitate efficient formation of multiple low- affinity adhesive interactions with hydrophobic surfaces of foreign particles. The polyvalent adhesive interactions can also be achieved via electrostatic interactions. Glycosylated regions of mucin fibers are densely coated with negative charges, such that mucus can also bind with positively charged particles with the same affinity. Many polymers useful in development of drug/ gene delivery systems are either hydrophobic (eg. PLGA, Poly anhydride) or cationic in nature (eg. polyethylenimine, chitosan and polylysine). When they come in contact with a mucus layer, hydrophobic and anionic forces will prevent them from penetrating through

mucus. This is a big challenge in design of particulate drug and gene delivery systems (Norris 1997, Cone 1999, Kircheis 2001, Kumar 2002, Bala 2004, Pack 2005).

Hence, conventional particles get trapped into mucin fiber network. It is true that mucoadhesive particles can improve pharmacokinetics of therapeutics at mucosal surface when compared to free drug alone. However, it has important limitations. Since mucoadhesive systems are bound to the mucus layer, they are cleared with mucus within seconds to hours. Moreover, they are incapable of efficiently penetrating through the mucus layer to reach the epithelium (Chickering 1996 and Mathiowitz 1997).

For intracellular drug and gene delivery, and for long term drug delivery system, mucus penetration is the key (Suk 2008, Sam 2010, Tang 2010). When the surface characteristics of viruses , including poliovirus, Norwalk virus and human papilloma virus (HPV)were studied with reference to mucosal penetration characteristic by Cone 1999 and, there were three important observations noted: (1) Sufficiently large surface area, (2) high density of surface charge , both positively and negatively charged groups, leading to a densely charged yet net neutral surface. but neutral surface and (3) Hydrophilic surface. This observation provided motivation to the Hanes research Group to modify polymer surface chemistry by mimicking the essential surface properties of viruses that allow them to avoid mucoadhesion.

Prof Justin Hanes and his group have reported (Suh 2004, Suh 2005, Suh 2007, Lai 2007, Wang 2008, Lai 2009, Tang 2009) that PEGylation of polymer facilitate the mucus penetration. However, it was not obvious to prove the role of PEGylation in mucus penetration where many early researches reported PEG as muco-adhesive agent. PEG is an uncharged hydrophilic polymer routinely useful in pharmaceutics to improve systemic circulation (Allen 2004, Harris 2003). Some authors have reported PEG chain establishes adhesive interaction due to their ability to inter diffusive with mucus network (Huang 2000, Bures 2001) and undergo hydrogen bonding. These work mainly focused on PEG coating of hydrogel system (Lele 2000) where the characteristic size of gel is greater than the average mucus pore spacing and reported

PEG as muco-adhesive. A number of reports in last decades also indicated PEG to enhance the muco-adhesive properties of nano-particles (Fresta 2001, Giannavola 2003, Sezgin 2007, Yoncheva 2007) although the density of PEG coating was typically under characterized.

It is very unlikely that PEG changes the mucus characteristic to facilitate mucus penetration. Hanes group at Johns Hopkins University, MD conducted systematic studies on mucus penetrating ability of PEG coating and they concluded that a dense coating of low molecular weight PEG on hydrophobic polymer facilitated mucus penetration, where PEG acts as a shield to protect the particles from interacting with proteins in mucus and helps them for penetration (Lai 2009).

In addition to improving transport, PEGylation of nanoparticles may also enhance their stability in mucus. Stability is important when particles must diffuse through a thick layer of mucus in order to reach underlying cells. Sanders et al found that mucus components did not interact significantly with PEG-GL 67 lipoplexes and prior exposure to the mucus components did not reduce their gene transfer. Similarly, in vitro incubation of PEG- coated Poly Lactide nano particles in simulated gastric fluid demonstrated 9- fold higher chemical stability than Poly Lactide alone (Rowland 1980, Chia-Ming 1987).

B-PEG-PLA, a PEGylated PLA degrades in body over 30 days (Kulkarni 1966) and biotin label helps for protein conjugation. Along with mucus penetrating ability, one more advantage of protein conjugation with B-PEG-PLA was observed that there was no obvious change in protein activity after biotin labelling when evaluated with In-Direct ELISA (data shown in chapter 5). With this reference, we extend application of MPP in the biological areas where proteins were covalently conjugated with mucus penetrating particles (MPP). We also believed that surface presentation of antigens would be better recognized and interacted with APCs than the antigens encapsulated in the biodegradable particulate system. For surface presentation of antigens, the polymer must have biological ligand which can interact with antigens. Therefore, in the given study, Biotin-PEG-PolyLactide (B-PEG-PLA) biodegradable polymer was

synthesized and nano-particles in the size of 200 nm were prepared and proteins were covalently conjugated with these nanoparticles. In-vitro mucus penetration studies were conducted with these NPs conjugated with antigens.

6.3 Multiple Particle Tracking

In early 90's, Single Particle Tracking (SPT) was used for studies related to transport behavior of proteins and lipid across the cell membrane. Qain et al 1991 presented the theoretical basis of analyzing trajectories obtained by SPT. Andersen 1992 and Cherry 1994 utilized approach of SPT using fluorescently labeled particles. Subsequently, Multiple -particle tracking (MPT) was developed and its application extended in the studies of viscoelastic behavior of complex biological fluids and intracellular environment. MPT can be explained as a computer-enhanced video microscopy which is used to track the motion of proteins, lipids, particulate matters or heterogeneous materials in the cell/ tissue environment ex vivo. Individual molecules or small clusters are observed with a typical spatial resolution of tens of nanometers and a typical time resolution of tens of milliseconds.

In video microscopy (Inou'e 1986, 1989), there is use of a high-quality video camera or other fast camera attached to a research-quality microscope for the purpose of real-time or high-speed imaging of samples on a microscope stage. These images are recorded at regular intervals (often at "video rate" of 30 images per second), and the time-lapse sequence can be played back in the form of a movie. The term "video microscopy" originally referred to microscope imaging using true video (30 frames per second) but now generally refers to rapid time-lapse imaging techniques. Video microscopy is used frequently to image small structures that move rapidly within cells as well as movement of whole cells. This motion can be well quantitated, and in the case of fluorescence microscopy, the changes in fluorescent intensity (reflecting the local chemical environment of the fluorescent molecule or the number of fluorescent molecules) can be quantitated as well.

The goal of MPT data analysis is to use particle trajectories to characterize the mode of transport and diffusivity. This technique is valuable in obtaining data on how fast particles move in complex cell environment. This technology addresses issues highlighted below (Saxton and Jacobson 1997):

(a) How do particles move on the cell surface? To what extent does the motion of various particles deviate from pure diffusion? How is that motion controlled and what its function?

(b) Measurements of trajectories of individual particles in the plasma membrane of cells show a variety of types of motion. Brownian motion is observed, but many of the particles undergo non-Brownian motion, including directed motion, confined motion, and anomalous diffusion. The variety of motion leads to significant effects on the pharmacokinetics of site-directed drug delivery system. This observation addresses key issue in designing effective drug/ gene delivery system.

(c) How do the properties like visco-elasticity of cell environment, pH of various mucus layer and different pore size of mucus barrier affect the particle movement?

Nanometer-Scale particle tracking is possible because the center of a small particle can be located with a precision well below the wavelength of light. However, two overlapping/ close particles can not be resolved. According to Rayleigh criterion, if the particles are too close, the pair cannot be resolved; however, this unresolved pair is more intense than the single spot of particle (Schnapp 1988, Sheetz 1989 and Ghosh 1994).

For mobile particles, motion of particles during acquisition time of image is the limiting factor for spatial resolution. The acquisition time depends on the label. In our study we have used fluorescent label for the imaging and reduction of background fluorescence which is of key importance to achieve a sufficiently high signal-to-noise ratio (SNR) of the intrinsically weak single-molecule signals. The use of high numerical aperture lenses and low fluorescent particle concentrations are mandatory, because otherwise the fluorescence of out-of-focus particles complicates the detection of single particle in the focal plane (Saxton and Jacobson 1997).

6.4 Mode of Transport

The concept of time scale is critical in video microscopy. Time scale can be defined as the time over which particle is allowed to move before calculating displacement from its initial point. Camera generally captures images at 30 frames/ second. The time interval between each frame would be 33 milli seconds (ms). Thus, the changes in particle displacements from frame to frame can be calculated. A movie of 600 frames will have 599 displacement values. Squaring the 599 displacements and determining the mean value result in the mean- square displacement (MSD) at the time scale of 33 ms. The acquisition time is optimized for the given a sample. The next shortest time is 66 ms, where particles are given more time to move on longer time scales. It is logical that MSD value will increase (Suh 2005).

Particle tracking allows single particle resolution and when large number of single particle tracking is done, then time dependence of the MSD for each particle is different. It is possible to group particles on the basis of their displacement behaviour. This is major advantage of MPT which help us to define mode of transport of individual particle (Suh 2005).

Experimentally, for each trajectory of a particle, two-dimensional mean square displacement for every time interval was calculated. The formula for calculation of MSD is as follows:

$$< \Delta r^2(\tau) >= \frac{1}{n}\sum_{i=0}^{n}\left(\left[x(t+\tau)-x(t)\right]^2+\left[y(t+\tau)-y(t)\right]^2\right) \qquad (1)$$

Where $t = 0.0667*i$, $n = T/\tau - 1$ and T = the length of the movie.

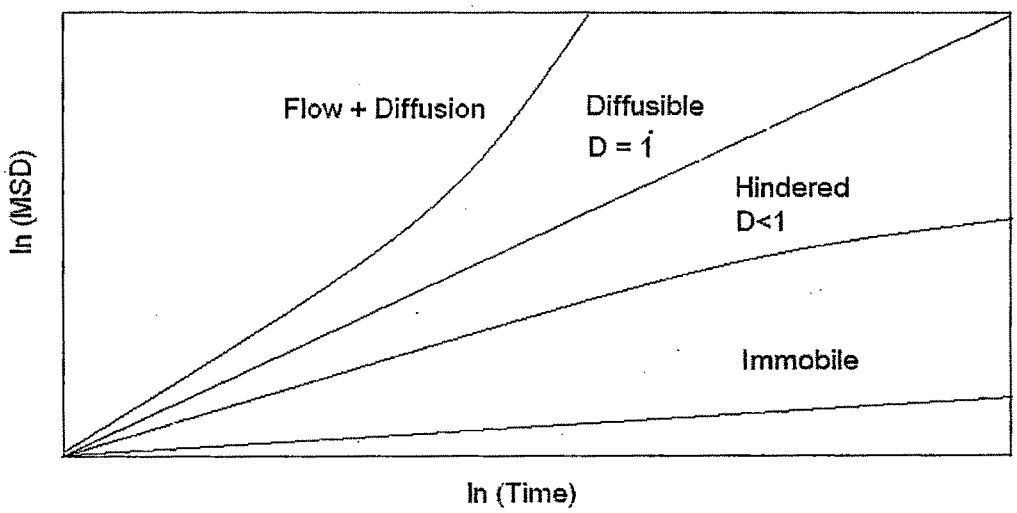

Figure 6.1 Times (mean square displacement) as a function for defining mode of transport

Coarsely, three modes of motions have been considered to describe the motional behaviour of particles: Stationary (Immobile), Diffusive and Hindered particles. Sub classification could also be possible if data cannot be fit to any one kind of behaviour due to sub-diffusive movement or Directed/ Active movement (Kusumi 1993, Saxton and Jacobson 1997, Suh 2003).

6.4.1 Diffusion

The MSD of diffusive particles is directly proportional to time. For simple diffusion, slope of the line is one (refer figure 6.1). The mathematical formula for this case can be written with Stokes- Einstein relation:

$\{(\Delta r^2(\tau)\} = 4 D_0 \tau,$ (2)

$\Delta r^2(\tau) = MSD$ (3)

$\ln (MSD) = \ln 4D_0 + \ln \tau$ and slope = 1

D_0 = Diffusion coefficient, τ = time

Value of Do can be obtained by fitting MSD v/s Time curve to a linear function. The particles that do not meet these criteria need to be sub-classified with the term- sub-diffusive particles (Dawson 2003).

Sub-diffusive mode of transport can be described mathematically as:

$$\{(\Delta r^2(\tau)\} = 4 D_0 \tau^{\alpha} \quad (4)$$

Where α is the anomalous coefficient and is equal to 1 for simple diffusion and less than 1 for sub-diffusive mode of transport. This transport mode can be due to the physical hindrance of the particles.

Directed or Active transport of particles can be described mathematically as:

$$\{(\Delta r^2(\tau)\} = 4 D_0 \tau + v^2 \tau^2 \quad (5)$$

Where v is the mean nano-complex velocity.

The values of D and v can be obtained by fitting the MSD v/s τ curve to a polynomial. Sometime, convection-directed transport is observed in a non-biological system which gives more or less similar data as Active transport (Suh 2003).

6.4.2 Hindered

Here particles undergo Brownian diffusion within a limited area and cannot move out of that area during the observation time. This mode generally occurs when particles get trapped within the flexible fiber network. By Fitting MSD v/s τ curve by least square analysis, it is possible to obtain the diffusion coefficients and transport velocity for this type (Suh 2004).

6.4.3 Immobile (Stationary mode)

Particles/ biological materials/ gene vectors show little or no motion during the speculated time which may be defined as Immobile or stationary mode of transport. In this mode of transport, particles are either sterically trapped or they adhere to the system (Suh 2004).

6.5 Experimental Technique

6.5.1 Requirement

Control Particles:

For the calibration of particles movements, two control particles were used:

one was carboxylate- Polystyrene (**PS-COOH**), where in the hydrophobic PS adheres to hydrophobic mucus patches and represent immobile particle group. 200nm size of PS-COOH particles were purchased from Invitrogen, FluoSphere, caboxylated-modified- Poly Styrene, yellow green fluorescent (505-515 emission-excitation maxima) 1 mL, 2% solids.

Second was PEGylated Polystyrene (**PS-PEG**). These particles were modified PS-COOH particle; modification was done at the Hanes laboratory. A standard protocol was followed for modification where there was involvement of standard EDC dehydration chemical reaction between amine group of PEG and carboxyl group of PS-COOH (Lai 2007). Other functional groups and chemistries may also be used. PS-PEG was the representative of diffusive particles.

Collection of Mucus samples

Mucus sample was used for these studies. Undiluted cervicovaginal mucus (CVM) from healthy female (age group 18-45) with normal vaginal flora were obtained using self sampling menstrual collection device following protocol approved by the Institutional Review Board of the Johns Hopkins University. The device was inserted into the vagina for 60 s, removed and placed into a 50 mL tube. Samples were centrifuged at 1000 rpm for 2 minutes to collect secretions (Tang 2009). The CV mucus generally has an acidic pH ~4, while respiratory mucus is near neutral in pH. Just before the use, the pH of the sample was determined by pH meter and adjusted to pH ~ 7 with Sodium Hydroxide (NaOH). Not more than 15% NaOH was added to the mucus sample to avoid unnecessary dilution.

Fluorescent labeling

The particles were labeled with fluorescent molecular probe, Rhodamine Red™-X conjugate of NeutrAvidin® (cat # 6378) from Invitrogen, USA.

The nano particles were prepared by single emulsion technique. These NPs (10 mg) were suspended in 750 µL of PBS. 750 µL of an aqueous solution of 200 µg/mL avidin rhodamin was added and incubated for 30 minutes at 37° C. Particles were collected by centrifugation and washed three times in PBS. Subsequently, particles were conjugated with Biotinylated protein as described in the chapter 5.

6.5.2 Sample Preparation for Microscopy

Once the fluorescent labeling of particle, mucus sample and controlled particles were ready, the samples for the video microscopy were prepared. The procedure for preparation of slides is described in Tang 2010 which is noted here in brief: quickly but gently, particle suspension of about 3-5% v/v was transferred to the mucus sample slides having about 30 μL of mucus sample followed by gentle stirring. Immediately it was sealed with a cover slip. To seal with cover slip, equal pressure at all corners was applied simultaneously to avoid air entrapment. Samples were then incubated at 37° C for 1-2 hours in 100% humid chamber to ensure sample do not dry out during incubation. At least 2 hours of incubation time before imaging is desirable to allow the mucus sample to equilibrate and to eliminate convection.

6.5.3 Video Microscopy

The video microscopy system comprised of Inverted epifluorescence microscope, Zeiss Axiovert 100 LM equipped with I-Pentamax 512 digital camera was used for the study. Before setting up actual experiments with the microscope, training was given by experts at Integrated Imaging Centre, Johns Hopkins University, Baltimore, USA.

6.5.4 Software for Data Analysis

MetaMorph 6.1 (Universal Imaging, Glendale, WI) was used for acquisition of the stream and tracking the single particle. The data obtained were analysed with set of modified MATLAB routine developed at Hanes Lab. The MSD and diffusivity graphs were plotted with KaleidaGraph 4.1 of Synergy Software.

6.6 Protein conjugated Nano Particle Tracking in Mucus

Particle transport rates were measured by analyzing trajectories of fluorescent particles, recorded by using I-Pentamax 512 digital camera mounted on an Inverted epifluorescence microscope equipped with 100X oil-immersion objective (N.A., 1.3). The movie for each test sample Antigen 85B (Ag85B) conjugated biotin-PEG-PLA

Nano Particles (B-PEG-PLA NP) with and without adjuvant, Dimethyl-diocadecylammonium bromide (DDAB) and Early secretory Antigen Target (ESAT-6) conjugated B-PEG-PLA NP with and without adjuvant DDAB along with both the controls, diffusive particle control (PS-PEG) and immobile particle (PS-COOH) were recorded with Metamorph software (Universal Imaging, Glendale, WI) at temporal resolution of 67 ms for 20 s. 540-507/ 529 nm (Rhodamine filter) was selected on the basis of emission/excitation maxima of each sample (information was taken from http://www.jhu.edu/iic/fluorophore.htm). The tracking resolution was 10 nm, determined by tracking displacements of particle immobilized with strong adhesive (Suh 2004). The coordinates of nano particles centroids were transformed into time averaged MSD. The formula for calculation of MSD is as follows,

$$\text{MSD or} < \Delta r^2(\tau) >= \frac{1}{n}\sum_{i=0}^{n}\left(\left[x(t+\tau)-x(t)\right]^2+\left[y(t+\tau)-y(t)\right]^2\right), \quad (6)$$

where $t = 0.0667*i$, $n = T/\tau - 1$ and T = the length of the movie where $\tau = 0.0667$ s and for a 20 s movie, there were a total of 300 frames and 299 displacements (n) with a time terval of τ. Pixel conversion was used to obtain unit of squared distance for MSD. The effective diffusivity (D_{eff}) as a function of time (τ) for each particle was calculated using formula (7) given by,

$$D_{eff} = MSD/(4\tau) \quad (7)$$

6.7 Particle Transport rate classification

The mode of transport (ie, diffusive, sub-diffusive, or immobile) of the nanoparticles was determined by calculating Relative Change (RC) for each particle. RC is defined as

$$RC = \frac{Deff, probed\ \tau}{Deff, reference\ \tau} \quad (8)$$

where the reference time scale is smaller than the probed. Therefore, RC is a measure of the relative change in diffusivity (Deff) of a single particle over time scale. In

theory, particles moving by simple diffusion are expected to have constant diffusivities over time scale (or a RC value of 1). Deff values increasing with time scale (RC values greater than 1) indicate directed or active transported particles, and Deff values decreasing with time scale (or RC values less than 1) suggest sub-diffusive particles (Dawson 2003; Suh 2003, 2004, 2005).

From data ensemble, an averaged of MSD and D_{eff} (averaged over all particles) were calculated. Based on these averaged values, transport mode classifications (% immobile, % hindered, and % diffusive) were determined. The following criteria were considered for the classification mode of transport.

Based on a Monte Carlo simulation of the distribution of RC values for purely Brownian particles, it was found that 95% of particles have RC_{short} values between (0.729897, 1.31238) and RC_{long} values between (0.725285, 1.25291). Particles with either RC_{short} or RC_{long} values below the upper limit were classified as hindered, while all other particles were classified as diffusive. Particles with MSDs below the spatial resolution of the microscope were classified as immobile (Suh 2003).

6.8 Results and Discussions

Various types of particles including two controls PS-PEG, a representative of diffusive particles and PS-COOH, a representative of Immobile particles, two proteins ESAT-6, a 9.8 kDa protein and Ag 85B, a 32 kDa protein conjugated to B-PEG-PLA NPs fabricated with and without DDAB were studied for mucus penetration. Data represent the ensemble average of at least three independent experiments, with $n \geq 90$ particles for each experiment and average n = 153, 169, and 120 for PS-PEG, PS-COOH and protein conjugated B-PEG-PLA MPP, respectively. For each experiment, the transport rates of particles were measured in the same sample. Data shown in table 6.1 is in the form of percentage. Figure 6.2 is the plot indicated transport mode for various types of particles.

Mode of Particle Transport	PS-PEG Control Particles-Diffusive	PS-COOH Control Particle immobile	ESAT-6 conjugated B-PEG-PLA-NP with DDAB	ESAT-6 conjugated B-PEG-PLA-NP	Ag 85B conjugated B-PEG-PLA-NP with DDAB	Ag 85B conjugated B-PEG-PLA-NP
Diffusive	100	6.39 ± 0.65	83.17 ± 7.6	74.46 ± 7.5	73.30 ± 5.7	51.17 ± 5.4
Hindered/ Immobile	0	93.70 ± 0.65	16.82 ± 7.6	25.25 ± 7.5	26.70 ± 5.7	48.83 ± 5.4

Table 6.1 A comparison of particle transport mode for two different proteins conjugated to B-PEG-PLA Nano Particles with and without cationic surfactant DDAB

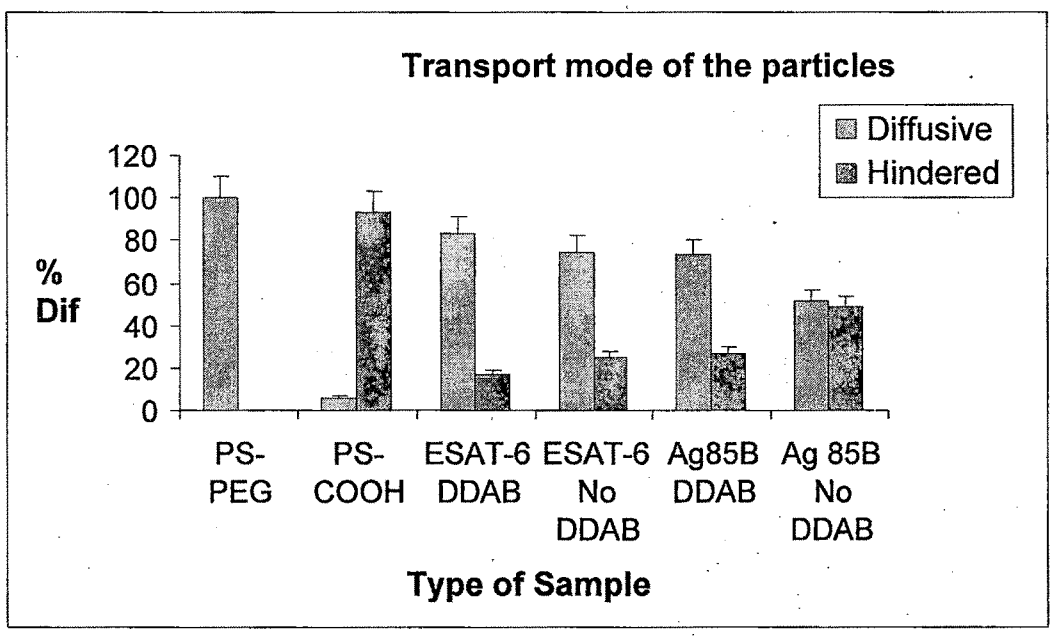

Figure 6.2 A comparison of particle transport mode for two different proteins conjugated to B-Peg-PLA Nano Particles with and without cationic surfactant DDAB

Trajectories of 150 particles were analysed by Metamorph software and MSD values were calculated with MATLAB routine and comparison of MSD values of both the protein conjugated NPs were made with control particles. The average ensemble MSD graphs were plotted with KaleidaGraph 4.1(Synergy Software), for Ag85 B conjugated to B-Peg-PLA fabricated with DDAB, Ag85 B conjugated to B-Peg-PLA fabricated without DDAB, ESAT-6 conjugated to B-Peg-PLA fabricated with DDAB and ESAT-6 conjugated to B-Peg-PLA fabricated without DDAB (data are not shown here).

Relative diffusivity of particles were averaged using Microsoft Excel software and one particles from all particles was selected with conditional formatting of all data and diffusivity plot for that particle were plotted by using KaleidaGraph 4.1 and it is as shown in figure 6.7. the data of mean square displacement was plotted against time in seconds (mS).

Figure 6.3, 6.4, 6.5 and 6.6 are the representative trajectories for 200 nm MPP with PS-PEG, PS-COOH and Protein conjugated B-PEG PLA (200nm NPs) where mean square Displacement (MSD) was plotted against ensemble average at a time scale of 1 s.

Figure 6.7 shows the trajectories of one representative particle from particles of the one group which was selected after analysing data for average value of the MSD.

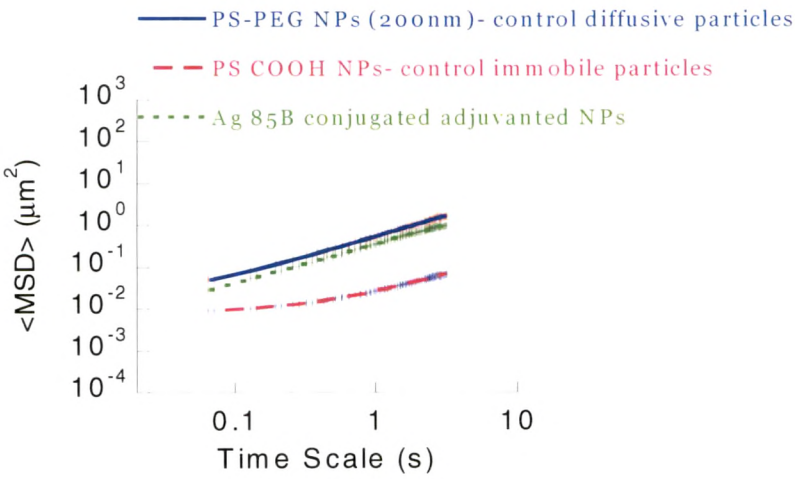

Figure 6.3 MSD plots for Ag85 B conjugated to B-Peg-PLA fabricated with DDAB

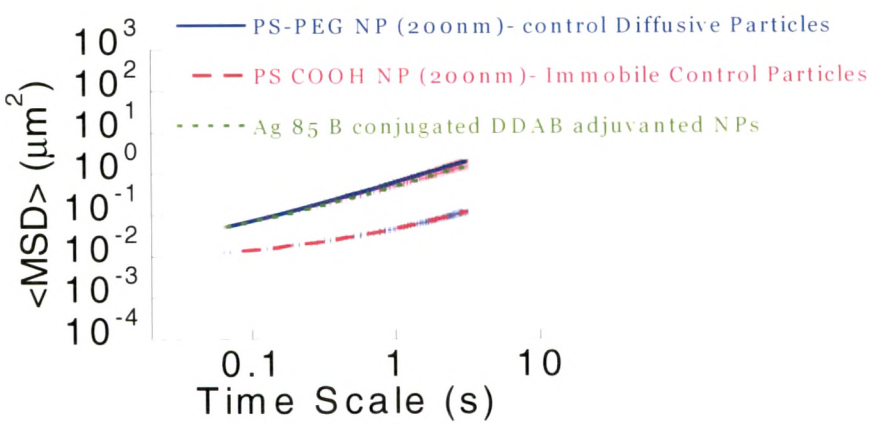

Figure 6.4 MSD plots for Ag85 B conjugated to B-Peg-PLA fabricated without DDAB

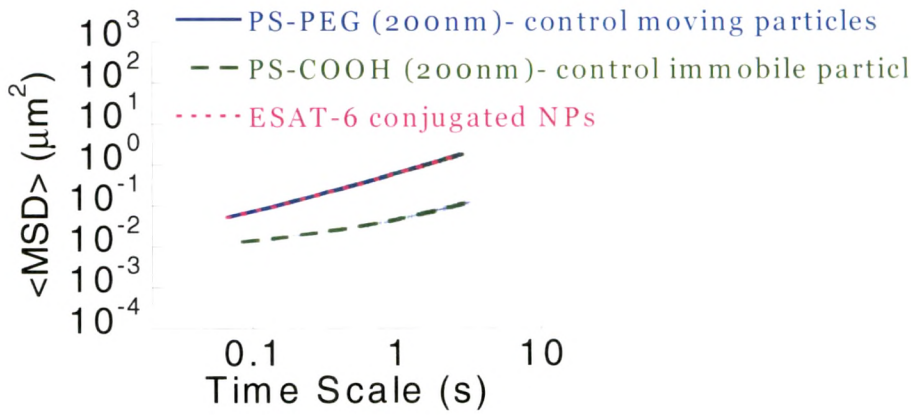

Figure 6.5 MSD plots for ESAT-6 conjugated to B-Peg-PLA fabricated with DDAB

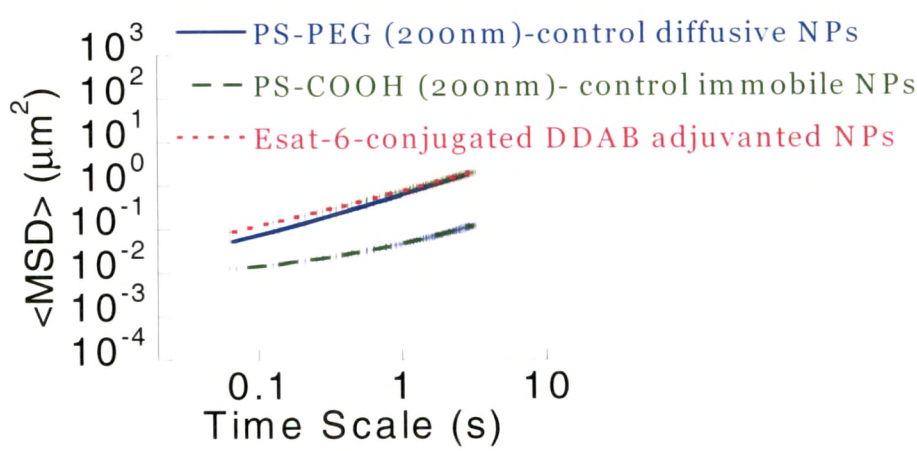

Figure 6.6 MSD plots for ESAT-6 conjugated to B-Peg-PLA fabricated without DDAB

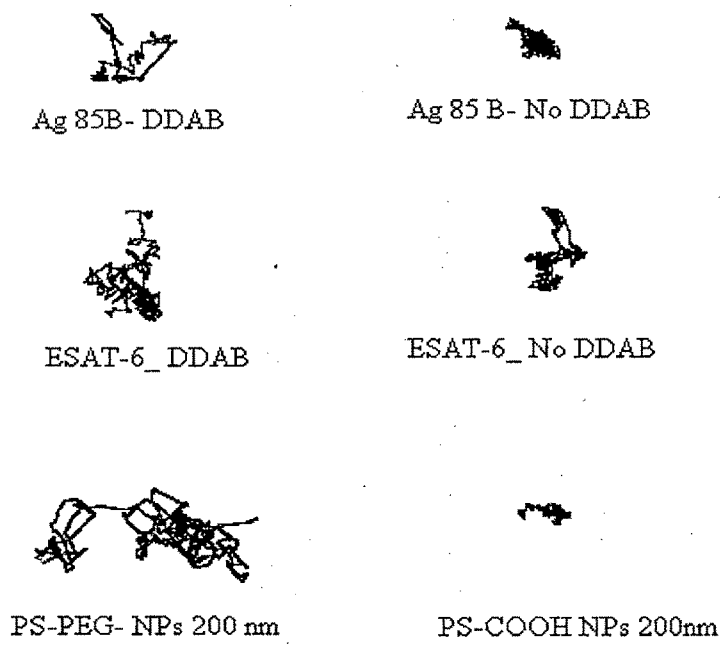

Figure 6.7 Diffusivity of Nano Particles in Mucus- control particles as well as test particles.

The present studies included recombinant proteins ESAT-6 (Skjot 2001) and Ag-85B (Sinha 1997, Yadav 2001 and Brooks 2001) which are strongly immunogenic and express in large amount during TB disease progression in the host (Orme 1993, Cooper 2002). To enable protein to reach APCs, we need to have delivery vehicles which also diffuse through mucus and hence mucus penetration studies were undertaken.

When mucus penetration of protein conjugated nano particles were studied in comparison with PS-COOH and PS-PEG, it was observed that ESAT-6 conjugated particles diffused faster (almost as similar to PS-PEG nano particles) in mucus than Ag-85B conjugated NPs. This observation can be justified as ESAT-6 (MW 6 kDa) is about 5-6 times smaller than Ag-85B (MW 32-34 kDa). The DDAB, which was added in the formulation as adjuvant to enhance immunogenicity of proteins, altered positively the proportion of particles diffusing through the mucus. This effect can be

justified with an argument that the surface charge of the particles is one of the governing factors in mucus penetration and near neutral particles diffuse through mucus very fast (Lai 2009). The amount of DDAB added during the fabrication process was optimized with this concept. Various proportion of DDAB was added during Nano particle synthesis (0.1 % w/w to 10% w/w). 5% w/w DDAB gave zeta potential around 3 ± 2 mV when compared to -5 ± 2 mV when no DDAB added.

Another noticeable finding of this experiment is a change in diffusive particles percentage in the case of Ag85B. A remarkable increase (from 51.17% to 73.30%) was found in diffusible particles when DDAB was added to the formulation. Several reports on study of Ag-85B indicated that Ag85B makes a complex with DDAB and this complex is responsible for enhance immunogenicity of Ag- 85B (Brandt 2000, Doherty 2002). This complex might be one reason for diffusive movement of Ag85B conjugated NPs in mucus even though with large molecular weight of the protein.

6.9 References

Ali, M.S., Pearson, J.P. (2007). Upper airway mucin gene expression: a review. *Laryngoscope*. **117,** 932–938.

Allen, T.M., Cullis, P.R. (2004). Drug delivery systems: entering the mainstream, *Science*, **303,** 1818–1822.

Anderson C.M., Georgiou G.N., Morrison I.E.G., Stevenson G.V.W., Cherry R.J. (1992). Tracking of cell surface receptors by fluorescence digital maging microscopy using a charge-coupled device camera. Low-density lipoprotein and influenza virus receptor mobility at 4^0C. *J. Cell Sci.* **101,** 415–25.

Bala, I., Hariharan, S., Kumar, M.N. (2004). PLGA nanoparticles in drug delivery: the state of the art. *Crit. Rev. Ther. Drug Carr. Syst.* **21,** 387–422.

Brandt L, Elhay M, Rosenkrands I, Lindblad EB, Andersen P (2002). ESAT-6 subunit vaccination against *Mycobacterium tuberculosis*. *Infect Immun*, **68(2),** 791–5.

Brooks, J.V., Frank, A.A., Keen, M.A., Bellisle, J.T., Orme, I.M. (2001). Boosting vaccine for tuberculosis. *Infect Immun*, **69(4),** 2714–7.

Bures, P., Huang, Y., Oral, E., Peppas, N.A. (2001). Surface modifications and molecular imprinting of polymers in medical and pharmaceutical applications. *J. Control. Release*, **72**, 25–33.

Cherry R.J., Georgiou G.N., Morrison I.E.G. (1994). New insights into the structure of cell membranes from single particle tracking experiments. *Biochem.Soc. Trans.* **22**, 781–84.

Chia-Ming, C., Weiner, N., (1987). Gastrointestinal uptake of liposomes. I. In vitro and in situ studies, *Int. J. Pharm.* **37**, 75–85.

Chickering, D., Jacob, J., Mathiowitz, E. (1996). Poly(fumaric-co-sebacic) microspheres as oral drug delivery systems, *Biotechnol. Bioeng.* **52**, 96–101.

Cone, R. (1999). Mucus, in: W.S. Michael, E. Lamm, Jerry R. McGhee, Lloyd Mayer, Jiri Mestecky, John Bienenstock (Eds.), Mucosal Immunlogy, Academic Press, San Diego, 1999, pp. 43–64.

Cooper, A.M., Kipnis, A., Turner, J., Magram, J., Ferrante, J., Orme, I.M. (2002). Mice lacking bioactive IL-12 can generate protective, antigen-specific cellular responses to mycobacterial infection only if the IL-12 p40 subunit is present, *J. Immunol.* **168**, 1322–1327.

Corfield, A.P., Carroll, D., Myerscough, N., Probert, C.S. (2001). Mucins in the gastrointestinal tract in health and disease, *Front. Biosci.* **6**, D1321–1357.

Dawson, M., Wirtz, D., Hanes, J. (2003). Enhanced viscoelasticity of human cystic fibrotic sputum correlates with increasing microheterogeneity in particle transport. *J. Biol. Chem.* **278**, 50393– 50401.

Dekker, J., Rossen, J.W.A., Buller, H.A., Einerhand, A.W.C. (2002). The MUC family: an obituary, *Trends Biochem. Sci.* **27**, 126–131.

Doherty TM, Olsen AW, van Pinxteren L, Andersen P (2002). Oral vaccination with subunit vaccines protects animals against aerosol infection with *Mycobacterium tuberculosis*. *Infect Immun* , **70(6)**, 3111–21.

Fresta, M., Fontana, G., Bucolo, C., Cavallaro, G., Giammona, G., Puglisi, G. (2001). Ocular tolerability and in vivo bioavailability of poly(ethylene glycol) (PEG)-coated polyethyl-2-cyanoacrylate nanosphere-encapsulated acyclovir. *J. Pharm. Sci.* **90**, 288–297.

Galabert, C., Jacquot, J., Zahm, J.M., Puchelle, E. (1987).Relationships between the lipid content and the rheological properties of airway secretions in cystic fibrosis, *Clin. Chim. Acta*, **164**, 139–149.

Ghosh, R.N., Webb, W.W. (1994). Automated detection and tracking of individual and clustered cell surface low density lipoprotein receptor molecules. *Biophys.J.* **66**, 1301–18.

Giannavola, C., Bucolo, C., Maltese, A., Paolino, D., Vandelli, M.A., Puglisi, G., Lee, V.H., Fresta, M. (2003). Influence of preparation conditions on acyclovir-loaded poly-d,l-lactic acid nanospheres and effect of PEG coating on ocular drug bioavailability. *Pharm. Res.*, **20**, 584–590.

Gipson, I.K. (2001). Mucins of the human endocervix, *Front. Biosci.* **6**, D1245–1255.

Girod, S., Zahm, J.M., Plotkowski, C., Beck, G., Puchelle, E. (1992). Role of the physiochemical properties of mucus in the protection of the respiratory epithelium, *Eur. Respir. J.* **5**, 477–487.

Harris, J.M, Chess, R.B. (2003). Effect of pegylation on pharmaceuticals, *Nat. Rev. Drug Discov.* **2**, 214–221.

Huang, Y., Leobandung, W., Foss, A., Peppas, N.A. (2000). Molecular aspects of muco- and bioadhesion: tethered structures and site-specific surfaces. *J. Control. Release*, **65**, 63–71.

Inou´e, S. (1986). *Video Microscopy.* New York: Plenum.

Inou´e, S. (1989). Imaging of unresolved objects, superresolution, and precision of distance measurement with video microscopy. *Methods Cell Biol.* **30**, 85–112.

Kircheis, R.L.W, Wagner, E (2001). Design and gene delivery activity of modified polyethylenimines. *Adv. Drug Deliv. Rev.* **53**, 341–358.

Kumar, N., Langer, R.S., Domb, A.J. (2001). Polyanhydrides: an overview. *Adv. Drug Deliv.Rev.* **54**, 889–910.

Kulkarni, P.K., Pani, P.C., Newman, C., Leonard, F. (1996). PolyLactic Acid for surgical implants. *Arch, Surg*, **93**, 839-844.

Kusumi, A., Sako, Y., Yamamoto, M. (1993). Confined Lateral Diffusion of Membrane Receptors as Studied by Single Particle Tracking (Nanovid Microscopy). Effects of Calcium-induced Differentiation in Cultured Epithelial Cells. *Biophysical Journal*, **65**, 2021-2040.

Lai, S.K., Elizabeth, O.T., Harrold, S., Man, S.T., Wang Y.Y.,Cone, R., Hanes, J. (2007) Rapid transport of large polymeric nanoparticles in f,resh undiluted human mucus. *Proc Natl Acad Sci USA* **104**, 1482-1487.

Lai, S.K., Wang Y.Y., Hanes, J. (2009). Mucus-penetrating nanoparticles for drug and gene delivery to mucosal tissues. *Advanced Drug Delivery Reviews* **61**, 158–171.

Lai, S.K., Wang, Y.Y., Hida, K., Cone, R., Hanes, J. (2010). Nanoparticles reveal that human cervicovaginal mucus is riddled with pores larger than viruses. *Proc Natl Acad Sci U S A*, 107(2), 598-603.

Lele, B.S., Hoffman, A.S. (2000). Mucoadhesive drug carriers based on complexes of poly (acrylic acid) and PEGylated drugs having hydrolysable PEG-anhydride-drug linkages, *J. Control. Release*, **69**, 237–248.

Mathiowitz, E., Jacob, J.S., Jong, Y.S., Carino, G.P., Chickering, D.E., Chaturvedi, P., Santos, C.A., Vijayaraghavan, K., Montgomery, S., Bassett, M., Morrell, C. (1997). Biologically erodable microsphere as potential oral drug delivery system, *Nature* **386**, 410–414.

Norris, D.A., Sinko, P.J. (1997). Effect of size, surface charge, and hydrophobicity on the translocation of polystyrene microspheres through gastrointestinal mucin. *J. Appl. Polym. Sci.* **63**, 1481– 1492.

Orme, I.M., (1993). Immunity to mycobacteria, *Curr. Opin. Immunol.* 5, 497–502.

Pack, D.W., Hoffman, A.S., Pun, S., Stayton, P.S. (2005). Design and development of polymers for gene delivery. *Nat. Rev. Drug Discov.* **4**, 581–593.

Qian H, Sheetz M.P., Elson E.L. (1991). Single particle tracking. Analysis of diffusion and flow in two-dimensional systems. *Biophys. J.* **60**, 910–21.

Raynal, B.D., Hardingham, T.E., Sheehan, J.K., Thornton, D.J. (2003). Calcium-dependent protein interactions in MUC5B provide reversible cross-links in salivary mucus. *J. Biol. Chem.* **278**, 28703–28710.

Rowland, R.N., Woodley, J.F. (1980). The stability of liposomes in vitro to pH, bile salts and pancreatic lipase, *Biochim. Biophys. Acta*, **620**, 400–409.

Rubin, B.K. (2002). Physiology of airway mucus clearance, *Respir. Care* **47**, 761–768.

Olmsted, S.S., J.L. Padgett, A.I. Yudin, K.J. Whaley, T.R. Moench, R.A. Cone, Diffusion of macromolecules and virus-like particles in human cervical mucus, *Biophys. J.* **81** (2001) 1930–1937.

Saltzman, W.M., Radomsky, M.L., Whaley, K.J., Cone, R.A. (1994). Antibody diffusion in human cervical-mucus. *Biophys. J.* **66**, 508–515.

Sanders, N.N., De Smedt, S.C., Cheng, S.H., Demeester, J., (2002). Pegylated GL67 lipoplexes retain their gene transfection activity after exposure to components of CF mucus, *Gene Ther.* **9**, 363–371.

Saxton M.J. and Jacobson K. (1997). Single-particle tracking: Applications to Membrane Dynamics. *Annu. Rev. Biophys. Biomol. Struct.* **26**, 373-399.

Schnapp, B.J., Gelles, J., Sheetz, M.P. (1988). Nanometer-scale measurements using video light microscopy. *Cell Motil.Cytoskel.* **10**, 47-53.

Sezgin, Z., Yuksel, N., Baykara, T., (2007). Investigation of pluronic and PEG-PE micelles as carriers of meso-tetraphenyl porphine for oral administration, *Int. J. Pharm.* **332**, 161–167.

Sheetz, M.P., Elson, E.L., (1993). Measurement of membrane glycoprotein movement by single-particle tracking. In *Optical Microscopy:Emerging Methods and Applications*, ed. B Herman, JJ Lemasters, pp. 285–94. San Diego: Academic Press

Singh, P.K; Parsek, M.R; Greenberg, E.P; Welsh, M.J. (2002). "A component of innate immunity prevents bacterial biofilm development". *Nature*, **417** (6888): 552–5.

Sinha, R.K., Verma, I., Khuller, G.K. (1997). Immunobiological properties of a 30 kDa secretory protein of *Mycobacterium tuberculosis* H37Ra. *Vaccine*, **15(6–7)**, 689–99.

Skjot, R.L., Oettinger, T., Rosenkrands, I., Ravn, P., Brock, I., Jacobsen, S. (2001). Comparative evaluation of low-molecular-mass proteins from *Mycobacterium tuberculosis* identifies members of the ESAT-6 family as immunodominant T-cell antigens. *Infect Immun*, **68(1)**, 214–20.

Suh, J., Choy, K.L., Lai, S.K., Tang, B.C., Prabhu, S., Hanes, J (2007). PEGylation of nanoparticles imporves their cytoplasmic transport. Intl. Jour. NanoMedicine, 2(4), 735- 741.

Suh, J., Dawson, M., Hanes, J. (2005). Real-time multiple-particle tracking: applications to drug and gene delivery. *Advanced Drug Delivery Reviews*, **57**, 63– 78.

Suh, J., Wirtz, D., Hanes, J (2003). Efficient active transport of gene nanocarriers to the cell nucleus. *Proc. Natl. Acad. Sci. U. S. A.*, **100**, 3878–3882.

Suh, J., Wirtz, D., Hanes, J (2004). Real-time intracellular transport of gene nanocarriers studied by multiple particle tracking. *Biotechnol. Prog.* **20**, 598– 602.

Tang, B.C., Dawson, M., Lai, S.K., Wang, Y.Y., Suk J.S.,Yang, M.,Zeitlin, P. ,Boyle, M.P., Fu, J. Hanes, J. (2009). Biodegradable polymer nanoparticles that rapidly penetrate the human mucus barrier. PNAS, **106**, 19268–19273.

Wolf, D.P., Blasco, L., Khan, M.A., Litt, M. (1977). Human cervical mucus. I. Rheologic characteristics. *Fertil. Steril.* **28**, 41–46.

Yadav, D., Khuller, G.K., (2001). Evaluation of immune responses directed against 30 kDa secretory protein of *Mycobacterium tuberculosis* H37Ra complexed in different adjuvants. *Indian J Exp Biol*, **39(12)**, 1227–34.

Yoncheva, K., Guembe, L., Campanero, M.A., Irache, J.M. (2007). Evaluation of bioadhesive potential and intestinal transport of pegylated poly(anhydride) nanoparticles. *Int.J. Pharm.* **334**, 156–165.

Reviewer's Comments

Reviewer's Comments